This is a preprint, the final version is subject to change, of the American Mineralogist (MSA)
Cite as Authors (Year) Title. American Mineralogist, in press.
(DOI will not work until issue is live.) DOI: http://dx.doi.org/10.2138/am.2014.4476

Revision_2

Neutron diffraction in gemmology:

Single-crystal diffraction study of brazilianite, $NaAl_3(PO_4)_2(OH)_4$

G. Diego Gatta[1], Pietro Vignola [1], Martin Meven[2,3], R. Rinaldi[4]

[1] Dipartimento di Scienze della Terra, Università degli Studi di Milano,
Via Botticelli 23, I-20133 Milano, Italy
[2]Institut für Kristallographie, RWTH Aachen, Jägerstrasse 17-19,
D-52056 Aachen, Germany
[3]Jülich Centre for Neutron Science – Outstation at FRM II, Lichtenbergstrasse 1,
D-85747 Garching, Germany
[4] Dipartimento di Scienze della Terra, Università degli Studi di Perugia,
Piazza Università 1, I-06123 Perugia, Italy

Abstract

The chemical composition and the crystal structure of a gem-quality brazilianite from the Telírio pegmatite, near Linópolis, Minas Gerais, Brazil, [$NaAl_3(PO_4)_2(OH)_4$, a = 11.2448(5) Å, b = 10.1539(6) Å, c = 7.1031(3) Å, β = 97.351(4)°, V = 804.36(7) Å^3, space group $P2_1/n$, Z = 4], have been reinvestigated by means of electron microprobe analysis in wavelength dispersive mode, single-crystal X-ray and neutron diffraction. The chemical analysis shows that brazilianite from Telírio Claim approaches almost ideal composition. The neutron anisotropic structural refinement was performed with final agreement index R_1 = 0.0290 for 211 refined parameters and 2844 unique reflections with Fo > 4σ(Fo), the X-ray refinement led to R_1 = 0.0325 for 169 refined parameters and 2430 unique reflections with Fo > 4σ(Fo). The building-block units of the brazilianite structure consist of chains of edge-sharing $AlO_4(OH)_2$ and $AlO_3(OH)_3$ octahedra. Chains are connected, via corner-sharing, by P-tetrahedra to form a three-dimensional framework, with Na atoms located in distorted cavities running along [100]. Five independent H sites were located, here labelled as H(1), H(2a), H(2b), H(3) and H(4). The configuration of the OH groups, along with the complex hydrogen bonding scheme, are now well defined. The O-H distances corrected for "riding motion"

range between ~0.992 Å and ~1.010 Å, the O···O distances between ~2.67 Å and ~2.93 Å, and the O–H···O angles between ~151° and ~174°. The H(2a) and H(2b) are only ~1.37 Å apart and mutually exclusive (both with site occupancy factor of 50%). The differences between the crystal structure of brazilianite and wardite (ideally $NaAl_3(PO_4)_2(OH)_4 \cdot 2H_2O$) are discussed. This work fulfils the need for accurate crystal chemical data for this gem mineral.

Key-words: brazilianite, crystal chemistry, single-crystal neutron diffraction, hydrogen bonding.

Introduction

Brazilianite, ideally $NaAl_3(PO_4)_2(OH)_4$, commonly forms equant to elongated monoclinic crystals with yellow to yellowish-green color, mainly found in large pockets in the *platy albite* (cleavelandite) units of granitic pegmatites. In granitic pegmatites, brazilianite is considered to form as a product of Na-metasomatic alteration of montebrasite-amblygonite. The type locality of this mineral, from which the name brazilianite, is the Corrego Frio pegmatite, Minas Gerais, Brazil, where it was first discovered in 1944 (Pough and Henderson 1945; Pecora and Fahey 1949). Brazilianite also occurs in phosphate-rich sedimentary deposits, *e.g.* Yukon Territories, Big Fish River, Stoneham Camp.

Brazilianite usually occurs in the form of perfect crystals (typically short prismatic, spearhead shaped, elongated along [100], usually with {011}, {$\bar{1}11$}, {010}, {110}, {$\bar{1}01$}, and {101}), grouped in druses and rarely as larger gem-quality crystals (Pough and Henderson 1945; Hurlbut and Weichel 1946; Frondel and Lindberg 1948; Pecora and Fahey 1949, Macrì 2011). The most important deposit of brazilianite is in

the surroundings of Conselheiro Pena, in the state of Minas Gerais. During the past few years, this deposit has yielded a great quantity of beautiful raw material, including dark greenish-yellow to olive-green crystals of surprisingly large dimensions (*i.e.* up to 10 cm in length and width) and perfectly bounded crystal faces. Crystals of similar shape and dimensions were discovered in another deposit in Minas Gerais, near Mantena. Minor deposits are those at the Palermo #1 Mine and G.E. Smith mine in New Hampshire, USA. Brazilianite is one of the few phosphate minerals to be used as a gemstone (along with amblygonite, turquoise and some gem varieties of apatite), and is relatively new to the gemstones market. The Mohs hardness of brazilianite is 5.5. The refraction indexes for the α, β, and γ rays are 1.602, 1.609 and 1.621-1.623, respectively. It is biaxial positive, with a birefringence of 0.019-0.021, and the dispersion is low (O'Donoghue 2006).

Only a few studies have so far been devoted to the crystal chemistry of brazilianite (Frondel and Lindberg 1948, and references therein). Its crystal structure was solved by Gatehouse and Miskin (1974), on the basis of single-crystal X-ray diffraction data, in the space group $P2_1/n$, with a~11.23 Å, b~10.14 Å, c~7.10 Å, and β~97.4° (Z = 4). Its structure consists of chains of edge-sharing Al-octahedra linked by P-tetrahedra forming a three-dimensional network, with Na atoms located in cavities parallel to [100] (Fig. 1). In the structure model of Gatehouse and Miskin (1974), there are two different configurations of the Al-octahedra: *trans*-$AlO_4(OH)_2$ and *trans*-$AlO_3(OH)_3$.

The general structure model of brazilianite reported by Gatehouse and Miskin (1974) appears to be consistent. However, the refinement included anisotropic displacement parameters only for the cation sites. In addition, the positions of the four independent proton sites appear to be affected by high uncertainties, as expected for X-

ray refinements at that time, and the isotropic thermal parameters were not refined. This led to a poor description of the complex H-bonding scheme in the brazilianite crystal structure. In this light, the aim of the present study is a reinvestigation of the crystal structure and crystal chemistry of a natural brazilianite (from Telírio) at ambient temperature by means of single-crystal X-ray and neutron diffraction and electron microprobe analysis in wavelength dispersive mode, in order to provide: *a*) the reliable location of the proton sites and the real topological configuration of the OH-groups, for a full description of the atomic relationship via the H-bonds; *b*) the anisotropic displacement parameters of all the atomic sites, H-sites included. This experiment follows a series of crystal structure investigations we have recently performed on gemstone minerals containing light elements (H, Li, Be, B) by single-crystal neutron diffraction (Gatta et al. 2010, 2012a, 2012b), a method offering definite advantages in these cases (Rinaldi et al. 2009).

Samples description and mineralogy

A prismatic single-crystal of pale yellow, gem-quality brazilianite (18 mm length and 5 mm width) from the Telírio pegmatite, near the village of Linópolis (not far from the Corrego Frio mine, type locality for brazilianite), in the Divino das Laranjeiras district (Minas Gerais, Brazil), was used for the chemical analysis and for the diffraction experiments of this study. The pegmatite field of East Minas Gerais is hosted by metamorphic rocks, belonging to the Precambrian shield, and consists of beryl- to complex-type granitic pegmatites, following the classification of Černý and Ercit (2005), which are rich in gemstones. Such pegmatites are mined by local miners (frequently a single mine, *garimpo*, is owned and mined by a single family of miners locally called *garimpeiros*) for gemstones (*e.g.* beryl, topaz, tourmaline). The Telírio

dike is a zoned pegmatite, with a well-developed Na-metasomatic unit and large pockets in cleavelandite containing brazilianite crystals up to 10 cm. The brazilianite crystal used in this study was perched on platy albite (3 x 3 x 2 cm of cleavelandite) and closely associated with zanazziite crystals (up to 3 mm).

Experimental methods

A preliminary check of the crystal of brazilianite chosen for this study was done under polarized light, showing that it was free of twinning, growth sectors or inclusions. The crystal was then cut into several pieces, in order to perform chemical analysis, X-ray and neutron diffraction experiments.

One fragment of the original single-crystal of brazilianite was used for the quantitative electron microprobe analysis in wavelength dispersive mode (EPMA-WDS) using a Jeol JXA-8200 electron microprobe at the Earth Science Department of the University of Milano (ESD-UMI). The crystal fragment was mounted in epoxy resin, polished and carbon coated. Major and minor elements were determined at 15 kV accelerating voltage, 5 nA beam current, and 3 μm beam diameter using a counting time of 30 sec on the peaks and 10 sec on the backgrounds. The following elements were analyzed: P, Al, Fe, Mn, Ba, Sr, Ca, Mg, Na, K, F and Cl, using a series of well characterized natural minerals as standards (graftonite for P, anorthite for Al, fayalite for Fe, rhodonite for Mn, barite for Ba, celestine for Sr, wollastonite for Ca, forsterite for Mg, omphacite for Na, K-feldspar for K, topaz for F and sodalite for Cl). The data were corrected for matrix effects using a conventional ΦρZ routine available in the Jeol suite of programs. A total number of 16 point analysis were performed, and the crystal was found to be homogeneous within the analytical error. The average chemical composition and the proportional formula are given in Table 1.

Two further fragments of the original large crystal, of approximately 4.2 x 3.6 x 2.8 mm^3 and 0.35 x 0.32 x 0.20 mm^3, were selected for the neutron and X-ray diffraction experiments, respectively. X-ray intensity data were collected at 293 K and up to $2\theta_{max} = 72.67°$ (with $-18 \le h \le 18$, $-13 \le k \le 13$ and $-11 \le l \le 11$, Table 2) with an Xcalibur diffractometer at the ESD-UMI, equipped with CCD, monochromatized Mo-$K\alpha$ radiation and operated at 50 kV and 40 mA. The data collection was performed with a combination of φ/ω scans, step size of 1° and an exposure time of 5 s/frame. A total number of 20604 Bragg reflections (with a high degree of redundancy) were collected, giving a metrically monoclinic unit-cell with: a = 11.2448(5), b = 10.1539(6), c = 7.1031(3) Å, β = 97.351(4)° and V = 804.4 $Å^3$ (Table 2). The systematic absences suggested the space group $P2_1/n$, as previously reported by Gatehouse and Miskin (1974). The intensity data were then integrated and corrected for Lorentz-polarization effects, using the computer program CrysAlis (Agilent Technologies 2012). An analytical absorption correction was applied by Gaussian integration based upon the physical description of the crystal (CrysAlis, Agilent Technologies 2012). After the corrections, the discrepancy factors among symmetry-related reflections (Laue class: $2/m$) was $R_{int} = 0.0392$ (Table 2).

The single-crystal neutron diffraction experiment was performed using the hot source (fast neutrons) single-crystal diffractometer HEiDi of the neutron source Forschungs-Neutronenquelle Heinz Maier-Leibnitz (FRM II). The diffraction data were collected at 293 K, with a wavelength of the incident beam of 0.7935(2) Å. A ^{3}He single counter detector was used [Eurisys 73NH17/5X end window counter, 50 mm entrance window, 5 bar ^{3}He pressure and 170 mm active length for high detection probability (>99% at 1.0 Å), separation of γ radiation by pulse height discrimination]. The unit-cell parameters were refined on the basis of the 40 Bragg reflections. A total number of

6321 reflections were collected (with $-18 \leq h \leq 18$, $-16 \leq k \leq 16$ and $-11 \leq l \leq 11$, rocking (= ω) scans below and ω/2θ scans above $2\theta = 55°$, $2\theta_{max} = 80.07°$, Table 2). The reflection conditions agreed with the space group $P2_1/n$. Integrated intensities were then corrected for Lorentz effect, and no absorption correction was applied, because of the shape and the dimensions of the sample. The discrepancy factor for the symmetry related reflections was $R_{int} = 0.0261$. Further details of the data collection are reported in Table 2.

Structure refinements

The X-ray intensity data of brazilianite were first processed with the program E-STATISTICS, implemented in the WinGX package (Farrugia 1999). The Wilson plot and the statistics of distributions of the normalized structure factors (*E*'s) suggested that the structure of brazilianite is centrosymmetric at 84.3 % likelihood. On this basis, and considering the reflections conditions, the anisotropic crystal structure refinement was then performed in the space group $P2_1/n$ using the SHELX-97 software (Sheldrick 1997, 2008), starting from the structure model of Gatehouse and Miskin (1974). The neutral scattering factors of Na, Al, P, O, and H were used according to the *International Tables of Crystallography* (Wilson and Prince, 1999). The secondary isotropic extinction effect was corrected according to Larson's formalism (1967), as implemented in the SHELXL-97 package (Sheldrick 1997, 2008). The first cycles of refinement were conducted without any H site. When convergence was achieved, no significant correlation was observed among the refined parameters in the variance-covariance matrix. All the principal mean square atomic displacement parameters were positively defined. The last cycles of refinement were conducted adding the H-sites on the basis of the neutron structure refinement (see below), and their coordinates were not

209 refined. At the end of the last cycle of refinement, no peak larger than +0.4/-0.4 *e*-/Å^3
210 was present in the final difference-Fourier map of the electron density (Table 2). The
211 final agreement index (R_1) was 0.0325 for 169 refined parameters and 2430 unique
212 reflections with $Fo>4\sigma(Fo)$ (Table 2). Site positions and displacement parameters (U_{ij})
213 are reported in Table 3a. Principal root-mean-square components of the atomic
214 displacement parameters are given in Table 4a. Bond lengths and angles are listed in
215 Tables 5.

216 The single-crystal neutron diffraction data of brazilianite were first processed
217 following the same protocol described for the X-ray data. The structure was found to be
218 centrosymmetric at 96.2 % likelihood. The anisotropic structure refinement was then
219 performed in the space group $P2_1/n$ using the SHELX-97 software (Sheldrick 1997,
220 2008), starting from the atomic coordinates of the model of Gatehouse and Miskin
221 (1974) without any H site. The neutron scattering lengths of Na, Al, P, O, and H were
222 used according to Sears (1986). The secondary isotropic extinction effect was corrected
223 according to Larson (1967). When convergence was achieved, five intense negative
224 residual peaks were found in the final difference-Fourier map of the nuclear density. As
225 hydrogen has a negative neutron scattering length, further refinement cycles were then
226 performed assigning H to these residual peaks (*i.e.* H(1), H(2a), H(2b), H(3) and H(4)
227 sites; Fig. 2, Table 3b). The final least-square cycles were conducted with anisotropic
228 thermal parameters for all sites (H-sites included). The convergence was achieved with
229 all the principal mean square atomic displacement parameters positively defined. The
230 variance-covariance matrix showed no significant correlation among the refined
231 parameters at the end of the refinement. No peak larger than +0.9/-0.9 fm/Å^3 was
232 present in the final difference-Fourier map of the nuclear density (Table 2). The final
233 agreement index (R_1) was 0.0290 for 211 refined parameters and 2844 unique

234 reflections with $F_o > 4\sigma(F_o)$ (Table 2). Atomic positions and displacement parameters
235 (U_{ij}) are listed in Table 3b. Principal root-mean-square components of the atomic
236 displacement parameters are given in Table 4b. Bond lengths and angles are listed in
237 Tables 5.
238
239 **Discussion and Conclusions**
240 The EPMA-WDS analysis shows that our sample of brazilianite from Telírio
241 approaches an almost ideal composition (*i.e.* $NaAl_3(PO_4)_2(OH)_4$). Na can partially be
242 replaced by K (or Ca). Some Fe^{3+} and Mg may replace Al at the octahedral sites (Table
243 1).
244 The single-crystal X-ray and neutron structure refinements of this study confirm
245 the general structure model of brazilianite described by Gatehouse and Miskin (1974).
246 The building-block units of the brazilianite structure consist of chains of edge sharing
247 *trans*-$AlO_4(OH)_2$ (*i.e.* around Al(2)) and *trans*-$AlO_3(OH)_3$ (*i.e.* about Al(1) and Al(3))
248 octahedra. The two chains are connected, via corner-sharing, by P-tetrahedra to form a
249 three-dimensional framework, with Na atoms located in distorted cavities running along
250 [100] (Fig. 1). The Na-polyhedron, here described with a coordination number of 9
251 (with $Na\text{-}O_{max} \sim 3.11$ Å; Fig. 2, Table 5), is strongly distorted. Gatehouse and Miskin
252 (1974) suggested that the distortion of the Na-polyhedron might be due to the H sites in
253 the [100]-cavity: the effect of mutual repulsion forces the Na site to one side of the
254 cavity, leading to a stronger Na-O interaction with oxygen sites on one side of the cavity
255 than on the other. This can now be confirmed by our neutron structure refinement, since
256 Na – H(4) distance is ~3.06 Å, Na – H(3) is ~3.16 Å and Na – H(2) is ~3.21 Å, and
257 H(4), H(3) and H(2) lie on the same side of the cavity. Both the X-ray and neutron
258 structure refinements show that the Al-octahedra appear to be significantly distorted,

with Δ[Al(1)-O]$_{max}$ ~ 0.32 Å, Δ[Al(2)-O]$_{max}$ ~ 0.31 Å, and Δ[Al(3)-O]$_{max}$ ~ 0.17 Å (*i.e.* the difference between the longest and the shortest Al-O distances, based on the X-ray structure refinement) (Table 5). The longest Al-O bond distances are those with the bridging oxygen shared between two Al-octahedra and one P-tetrahedron (*i.e.* O(6) and O(7), Table 5). The shortest Al-O bond distances are those with oxygen atoms of OH-groups (*i.e.* O(1), O(2), O(3) and O(4), Table 5). P-tetrahedra appear to be less distorted, as Δ[P(1)-O]$_{max}$ ~ 0.044 Å and Δ[P(2)-O]$_{max}$ ~ 0.036 Å (*i.e.* the difference between the longest and the shortest P-O distances, based on the X-ray structure refinement) (Table 5).

The neutron structure refinement of this study provides an unambiguous location of the H-sites, allowing the description of the H-bonding scheme in the brazilianite structure. Five independent H sites were located, here labelled H(1), H(2a), H(2b), H(3) and H(4). The configuration of the OH groups (*i.e.* O(1)–H(1), O(2)–H(2a), O(2)–H(2b), O(3)–H(3), O(4)–H(4)), along with the hydrogen bonding scheme, are now well defined (Fig. 2, Table 5). O(1), O(2), O(3) and O(4) act as *donors*, whereas O(2), O(4), O(9) and O(12) as *acceptors*. Symmetry-related O(2) act both as *donor* and as *acceptor* of H-bonds. The O-H distances corrected for "riding motion" (Busing and Levy 1964), range between ~0.992 Å and ~1.010 Å, the O···O distances between ~2.67 Å and ~2.93 Å, and the O–H···O angles between ~151° and ~174° (Table 5). The H(2a) and H(2b) are only ~1.37 Å apart. The neutron structure refinement was carried out without any restraint on the site occupancy factors (*s.o.f.*) of H(2a) and H(2b), leading to *s.o.f.*(H2a) = 0.546(6) and *s.o.f.*(H2b) = 0.446(6), respectively (Table 3b). We can thus consider a general *s.o.f.* of 50% each for H(2a) and H(2b), therefore the two H-sites are mutually exclusive. Additional test refinements were performed in order to check if this H-site splitting reflects a lower symmetry than $P2_1/n$, but without success. The key to

understand the splitting of H(2a) and H(2b) in two mutually exclusive sites is in the H-bonding scheme of the structure. In fact, if only one "virtual" H(2) site should occur, located between H(2a) and H(2b), it would have an energetically unfavourable H-bond configuration, with O(2)-H(2)···O(9) ~ 113° and O(2)-H(2)···O(2) ~ 127°, whereas the split site configuration yields O(2)-H(2a)···O(9) ~ 151° and O(2)-H(2b)···O(2) ~ 171° (Table 5).

The principal root-mean-square components of the atomic displacement parameters of the H sites show a slightly pronounced anisotropy, in particular for the H(2b) and H(3) sites (Table 4b). Both the X-ray and the neutron structure refinements show that: *a*) the Na site has the highest displacement anisotropy, about the equilibrium position, among the cation sites, and *b*) O(5), O(8), O(9) and O(10) sites have the highest anisotropy among all the oxygen sites, and they are all bridging oxygen between P-tetrahedra and Al-octahedra (Tables 4a, 4b and 5).

It is interesting to point out how the structure of brazilianite and that of wardite (ideally $NaAl_3(PO_4)_2(OH)_4 \cdot 2H_2O$, Fanfani et al. 1974) are significantly different, as highlighted by Gatehouse and Miskin (1974), despite the "chemical similarity". As in brazilianite, also in wardite the primary building units are P-tetrahedra and Al-octahedra. However, in wardite P-tetrahedra join the sheets of corner-linked Al-octahedra, whereas in brazilianite edge-sharing Al-octahedra occur. In wardite, H_2O is not "zeolitic": the molecule is coordinated to Al, and not to Na in the [100]-cavity. This leads to a different crystal structure of the two mentioned minerals.

Acknowledgements

The authors thank the Forschungsneutronenquelle Heinz Maier-Leibnitz (FRM II), München, Germany, for the allocation of beam time. Authors kindly thank Sergio Varvello, who provided the sample of brazilianite, and Andrea Risplendente, for his assistance during the EPMA analyses. W. Simmons, F. Hatert and the Associate Editor A. Celestian are thanked for the revision of the manuscript. This study was founded by the Italian Ministry of Education, MIUR-Project: 2010EARRRZ_003.

References

Agilent Technologies (2012) Xcalibur CCD system, CrysAlis Software system.

Busing W.R. and Levy H.A. (1964) The effect of thermal motion on the estimation of bond lengths from diffraction measurements. Acta Crystallographica, 17, 142-146.

Černý, P. and Ercit, S. (2005): The classification of granitic pegmatites revisited. Canadian Mineralogist, 43, 2005-2026.

Fanfani, L., Nunzi, A., and Zanazzi, P.F. (1970) The crystal structure of wardite. Mineralogical Magazine, 37, 598-605.

Farrugia, L.J. (1999) WinGX suite for small-molecule single-crystal crystallography. Journal of Applied Crystallography, 32, 837-838.

Frondel, C., and Lindberg, M.L. (1948) Second occurrence of brazilianite. American Mineralogist, 33, 135–141.

Gatehouse, B.M., and Miskin, B.K. (1974) The crystal structure of brazilianite, $NaAl_3(PO_4)_2(OH)_4$. Acta Crystallographica, 30, 1311–1317.

Gatta, G.D., Vignola, P., McIntyre, G.J., and Diella, V. (2010) On the crystal chemistry of londonite [(Cs,K,Rb)$Al_4Be_5B_{11}O_{28}$]: a single-crystal neutron diffraction study at 300 and 20 K. American Mineralogist, 95, 1467–1472.

Gatta, G.D., Danisi, R.M., Adamo, I., Meven, M., and Diella, V. (2012a) A single-crystal neutron and X-ray diffraction study of elbaite. Physics and Chemistry of Minerals, 39, 577–588.

Gatta, G.D., Adamo, I., Meven, M., and Lambruschi, E. (2012b) A single-crystal neutron and X-ray diffraction study of pezzottaite, $Cs(Be_2Li)Al_2Si_6O_{18}$. Physics and Chemistry of Minerals, 39, 829–840.

Hurlbut, C.S., and Weichel, J.W. (1946) Additional data on brazilianite. American Mineralogist (Notes and News), 31, 507.

Larson, A.C. (1967) Inclusion of secondary extinction in least-squares calculations. Acta Crystallographica, 23, 664 – 665.

Macrì, M. (2011) Brasilianite, una pietra luminosa che ha vissuto per lunghi secoli al buio. Rivista Gemmologica Italiana, 6-1, 24-26.

O'Donoghue, M. (2006) Gems, Sixth Edition. Butterworth-Heinemann, Elsevier, 873 pp. (ISBN-10: 0750658568).

Pecora, W.T., and Fahey, J.J. (1949) The Corrego Frio pegmatite, Minas Gerais: scorzalite and souzalite, two new phosphate minerals. American Mineralogist, 34, 83-93.

Pough, F. H., and Henderson, E.P. (1945) Brazilianite, a new phosphate mineral. American Mineralogist, 30, 572–582.

Rinaldi, R., Liang, L., Schober, H. (2009) Neutron Applications in Earth, Energy and Environmental Sciences. In L. Liang, R. Rinaldi and H. Schober, eds., Neutron

356 Applications in Earth, Energy and Environmental Sciences, pp. 1-14. Springer Science,
357 New York.

358 Sears, V.F. (1986) Neutron Scattering Lengths and Cross-Sections. In K. Sköld
359 and D.L. Price, Eds., Neutron Scattering, Methods of Experimental Physics, Vol. 23A,
360 p. 521-550. Academic Press, New York.

361 Sheldrick, G.M. (1997) SHELX-97. Programs for crystal structure determination
362 and refinement. University of Göttingen, Germany.

363 Sheldrick, G.M. (2008) A short history of SHELX. Acta Crystallographica, A64,
364 112-122.

365 Wilson, A.J.C., and Prince, E. (1999) International Tables for X-ray
366 Crystallography, Volume C: Mathematical, physical and chemical tables (2nd Edition),
367 Kluwer Academic, Dordrecht, NL.

368

Table and Figure captions

Table 1. Representative compositions of brazilianite from Telírio, based on EPMA-WDS analysis (16 data points). Formula proportions calculated on the basis of 2 atoms of P per formula unit (*a.p.f.u.*)

Table 2. Details of X-ray and neutron data collection and refinements of brazilianite.

Table 3a. Atomic coordinates and thermal displacement parameters ($Å^2$) of brazilianite based on the X-ray structure refinement. The anisotropic displacement factor exponent takes the form: $-2\pi^2[(ha^*)^2U_{11} + \ldots + 2hka^*b^*U_{12}]$. U_{eq} is defined as one third the trace of the orthogonalised U_{ij} tensor.

Table 3b. Atomic coordinates and thermal displacement parameters ($Å^2$) of brazilianite based on the neutron structure refinement. The anisotropic displacement factor exponent takes the form: $-2\pi^2[(ha^*)^2U_{11} + \ldots + 2hka^*b^*U_{12}]$. U_{eq} is defined as one third the trace of the orthogonalised U_{ij} tensor.

Table 4a. Principal root-mean-square components (R1, R2 and R3, x 10^2 Å) of the atomic displacement parameters based on the X-ray structure refinement.

Table 4b. Principal root-mean-square components (R1, R2 and R3, x 10^2 Å) of the atomic displacement parameters based on the neutron structure refinement.

Table 5. Relevant bond distances (Å) and angles (°) in the brazilianite structure based on the X-ray structure refinement (XSR) and the neutron structure refinement (NSR).

Fig. 1. Two views of the crystal structure of brazilianite (*i.e.* down [100] and [001]) based on the neutron structure refinement of this study. Thermal ellipsoid probability factor: 60%. Al-octahedra are in light grey, P-tetrahedra in dark grey, Na sites (medium grey) as un-bonded atoms, H-sites in white.

Fig. 2. Hydrogen sites location, H-bonding scheme and configuration of the Na-polyhedron in the structure of brazilianite based on the neutron structure refinement of this study. The sites H(2a) and H(2b) are mutually exclusive. Thermal ellipsoid probability factor: 60%.

406

407 Table 1. Representative compositions of brazilianite from Telírio, based on EPMA-
408 WDS analysis (16 data points). Formula proportions calculated on the basis of 2 atoms
409 of P per formula unit (*a.p.f.u.*)

410

411

	wt%	*e.s.d*	*Ions* (*a.p.f.u.*)	
P_2O_5	39.26	0.48	P	2.000
Al_2O_3	42.40	0.38	Al	3.007
Fe_2O_3	0.04	0.03	Fe^{3+}	0.002
MgO	0.04	0.03	Mg	0.003
SrO	0.05	0.05	Sr	0.002
CaO	0.03	0.01	Ca	0.002
Na_2O	8.18	0.18	Na	0.955
K_2O	0.01	0.01	K	0.001
H_2O*	9.41		OH-	4.001
Total	99.41			

Notes: * calculated on the basis of 4 OH^- *a.p.f.u.*. Mn, Ba, Cl and F below detection limit.

412

413

414

415

416

417

418

419

420

421

422

423

424

425

426

427

428

Table 2. Details of the X-ray and neutron data collection and refinements of brazilianite.

Crystal shape	Prismatic	Prismatic
Crystal size (mm^3)	4.2 x 3.6 x 2.8	0.35 x 0.32 x 0.20
Crystal colour	Translucent pink	Translucent pink
Unit-cell constants	a = 11.243(2)Å	a = 11.2448(5)Å
	b = 10.154(2)Å	b = 10.1539(6) Å
	c = 7.115(1)Å	c = 7.1031(3) Å
	β = 97.32(2)°	β = 97.351(4)°
Reference chemical formula	$NaAl_3(PO_4)_2(OH)_4$	$NaAl_3(PO_4)_2(OH)_4$
Space Group	$P2_1/n$	$P2_1/n$
Z	4	4
T (K)	293	293
ρ_{calc} ($g \cdot cm^{-3}$)	2.984	2.989
Radiation (Å)	Neutron, 0.7935(2)	X-ray, Mo-$K\alpha$
Diffractometer	HEiDi, four circle	XCalibur-CCD
Data-collection strategy:		
scan type	31 steps,	ω-φ scans
	ω-scan at $2\theta < 55°$	
	ω/2θ -scan at $2\theta \geq 55°$	
time per step (s)	5	5
width; u, v, q	5.4, -12.0, 16.3	1°
Max. 2θ (°)	80.07	72.67
	$-18 \leq h \leq 18$	$-18 \leq h \leq 18$
	$-16 \leq k \leq 16$	$-13 \leq k \leq 13$
	$-11 \leq l \leq 11$	$-11 \leq l \leq 11$
No. measured reflections	6321	20604*
No. unique reflections	3461	2968
No. unique refl. with $F_o > 4\sigma(F_o)$	2844	2430
No. refined parameters	211	169
R_{int}	0.0261	0.0392
R_1 (F) with $F_o > 4\sigma(F_o)$	0.0290	0.0325
R_1 (F) for all the unique refl.	0.0462	0.0548
wR_2 (F^2)	0.0474	0.0487
S	1.343	1.422
Weighting Scheme: a, b	0.01, 0	0.01, 0
Residuals (fm/ $Å^3$)	+0.9/-0.9	+0.4/-0.4

Note: $R_{int} = \Sigma|F_{obs}^2 - F_{obs}^2(mean)|/\Sigma[F_{obs}^2]$; $R_1 = \Sigma(||F_{obs}| - |F_{calc}||)/\Sigma|F_{obs}|$; $wR_2 = [\Sigma[w(F^2_{obs} - F^2_{calc})^2]/\Sigma[w(F^2_{obs})^2]]^{0.5}$, $w = 1/[\sigma^2(F_{obs}^2) + (aP)^2 + bP]$, $P = (\text{Max}(F_{obs}^2, 0) + 2*F_{calc}^2)/3$.
Neutron ω-scan width : $(u + v*\tan\theta + q*\tan^2\theta)^{0.5}$. *High degree of redundancy.

Table 3a. Atomic coordinates and thermal displacement parameters (Å^2) of brazilianite based on the X-ray structure refinement. The anisotropic displacement factor exponent takes the form: $-2\pi^2[(ha^*)^2U_{11} + \ldots + 2hka^*b^*U_{12}]$. U_{eq} is defined as one third the trace of the orthogonalised U_{ij} tensor.

	x/a	*y/b*	*c/z*	U_{eq}/U_{iso}	U_{11}	U_{22}	U_{33}	U_{12}	U_{13}	U_{23}
Na	0.30332(7)	0.07508(6)	0.03476(9)	0.0239(2)	0.0403(4)	0.0155(4)	0.0166(3)	-0.0053(3)	0.0065(3)	0.0006(3)
Al(1)	0.04325(4)	0.22069(4)	0.56161(5)	0.0058(1)	0.0063(2)	0.0066(2)	0.0046(2)	0.0002(2)	0.0015(1)	-0.0003(2)
Al(2)	0.26290(3)	0.06750(4)	0.50805(5)	0.0057(1)	0.0052(2)	0.0058(2)	0.0061(2)	0.0000(2)	0.0010(1)	-0.0005(2)
Al(3)	0.45940(4)	0.25420(4)	0.43268(5)	0.0055(1)	0.0058(2)	0.0061(2)	0.0047(2)	0.0001(2)	0.0015(1)	0.0005(2)
P(1)	0.18049(3)	0.31231(4)	0.23748(4)	0.00506(7)	0.0049(2)	0.0057(2)	0.0045(1)	0.0002(1)	0.0005(1)	0.0007(1)
P(2)	0.31236(3)	0.32791(4)	0.75393(4)	0.00478(7)	0.0050(2)	0.0050(2)	0.0044(1)	-0.0004(1)	0.0007(1)	-0.0005(1)
O(1)	0.10330(8)	0.07984(9)	0.44944(12)	0.0067(2)	0.0059(4)	0.0067(5)	0.0074(4)	-0.0003(4)	0.0003(3)	-0.0020(4)
O(2)	0.42379(8)	0.10107(9)	0.56258(12)	0.0073(2)	0.0068(4)	0.0078(5)	0.0073(4)	-0.0006(4)	0.0004(3)	0.0003(4)
O(3)	0.00300(8)	0.34973(9)	0.72421(12)	0.0072(2)	0.0082(4)	0.0069(5)	0.0070(4)	-0.0012(4)	0.0023(3)	-0.0014(4)
O(4)	0.49748(8)	0.38585(9)	0.26989(12)	0.0074(2)	0.0091(5)	0.0072(5)	0.0059(4)	-0.0004(4)	0.0012(3)	0.0004(4)
O(5)	0.11484(8)	0.23907(10)	0.06731(13)	0.0087(2)	0.0073(5)	0.0106(5)	0.0079(4)	0.0000(4)	-0.0009(3)	-0.0018(4)
O(6)	0.28766(8)	0.22135(9)	0.31813(12)	0.0071(2)	0.0068(4)	0.0075(5)	0.0070(4)	0.0001(4)	0.0007(3)	0.0007(4)
O(7)	0.22619(8)	0.21329(9)	0.68151(12)	0.0069(2)	0.0075(4)	0.0065(5)	0.0069(4)	-0.0010(4)	0.0013(3)	-0.0017(4)
O(8)	0.38755(8)	0.28025(10)	0.93465(12)	0.0080(2)	0.0067(4)	0.0107(5)	0.0064(4)	0.0000(4)	-0.0002(3)	0.0013(4)
O(9)	0.09990(8)	0.34050(9)	0.39257(12)	0.0077(2)	0.0081(4)	0.0077(5)	0.0080(4)	0.0011(4)	0.0037(3)	0.0007(4)
O(10)	0.39145(8)	0.36733(10)	0.60223(12)	0.0077(2)	0.0092(5)	0.0075(5)	0.0071(4)	-0.0016(4)	0.0037(3)	-0.0005(4)
O(11)	0.22579(8)	0.44660(9)	0.18273(12)	0.0088(2)	0.0105(5)	0.0081(5)	0.0080(4)	-0.0012(4)	0.0017(3)	0.0014(4)
O(12)	0.23569(8)	0.44836(9)	0.79031(12)	0.0075(2)	0.0071(4)	0.0072(5)	0.0081(4)	0.0010(4)	0.0003(3)	-0.0008(4)
H(1)	0.06558	0.01329	0.36283	0.058(7)						
H(2a)	0.46380	0.10177	0.69397	0.05(1)						
H(2b)	0.47657	0.02977	0.53443	0.07(2)						
H(3)	0.07059	0.40794	0.75715	0.052(6)						
H(4)	0.04861	0.04549	0.82972	0.078(8)						

Note: H-sites coordinates fixed to the values from the neutron structure refinement (Table 3b), their thermal parameters refined isotropically.

492 Table 3b. Atomic coordinates and thermal displacement parameters (Å^2) of brazilianite
493 based on the neutron structure refinement. The anisotropic displacement factor exponent
494 takes the form: $-2\pi^2[(ha^*)^2U_{11} + \ldots + 2hka^*b^*U_{12}]$. U_{eq} is defined as one third the trace
495 of the orthogonalised U_{ij} tensor.
496
497

	x/a	*y/b*	*c/z*	U_{eq}	U_{11}	U_{22}	U_{33}	U_{12}	U_{13}	U_{23}
Na	0.30320(11)	0.07526(10)	0.03507(15)	0.0230(2)	0.0378(5)	0.0152(4)	0.0168(4)	-0.0064(4)	0.0068(4)	0.0002(3)
Al(1)	0.04311(6)	0.22082(7)	0.56153(10)	0.0047(1)	0.0047(2)	0.0054(3)	0.0040(3)	0.0000(2)	0.0009(2)	-0.0010(2)
Al(2)	0.26289(6)	0.06763(7)	0.50793(10)	0.0041(1)	0.0029(2)	0.0047(3)	0.0048(3)	0.0000(2)	0.0005(2)	-0.0004(2)
Al(3)	0.45954(6)	0.25430(7)	0.43278(10)	0.0039(1)	0.0039(2)	0.0048(2)	0.0032(3)	0.0001(2)	0.0010(2)	0.0004(2)
P(1)	0.18042(4)	0.31237(5)	0.23765(7)	0.00359(7)	0.0029(2)	0.0046(2)	0.0032(2)	0.0003(1)	0.0000(1)	0.0004(1)
P(2)	0.31242(4)	0.32789(5)	0.75398(7)	0.00331(7)	0.0031(2)	0.0037(2)	0.0032(2)	-0.0004(1)	0.0006(1)	-0.0008(1)
O(1)	0.10308(4)	0.07987(4)	0.44925(6)	0.00550(7)	0.0032(1)	0.0062(2)	0.0069(2)	0.0003(1)	0.0000(1)	-.0026(1)
O(2)	0.42380(4)	0.10065(4)	0.56264(6)	0.00571(7)	0.0044(2)	0.0064(2)	0.0063(2)	-0.0007(1)	0.0004(1)	0.0017(1)
O(3)	0.00288(4)	0.35011(4)	0.72467(6)	0.00576(7)	0.0063(2)	0.0060(2)	0.0052(2)	-0.0005(1)	0.0016(1)	-0.0010(1)
O(4)	0.49766(4)	0.38570(4)	0.26966(6)	0.00549(7)	0.0062(2)	0.0060(2)	0.0044(2)	-0.0002(1)	0.0009(1)	0.0007(1)
O(5)	0.11452(4)	0.23958(5)	0.06717(7)	0.00685(7)	0.0050(2)	0.0098(2)	0.0052(2)	0.0001(1)	-0.0015(1)	-0.0019(1)
O(6)	0.28757(4)	0.22174(4)	0.31817(6)	0.00495(7)	0.0037(1)	0.0058(2)	0.0051(2)	0.0013(1)	-0.0003(1)	0.0003(1)
O(7)	0.22596(4)	0.21374(4)	0.68144(6)	0.00501(7)	0.0050(1)	0.0050(2)	0.0050(2)	-0.0015(1)	0.0007(1)	-0.0015(1)
O(8)	0.38765(4)	0.28028(4)	0.93474(7)	0.00668(7)	0.0047(2)	0.0097(2)	0.0051(2)	0.0004(1)	-0.0014(1)	0.0014(1)
O(9)	0.10001(4)	0.34063(4)	0.39249(7)	0.00635(7)	0.0068(2)	0.0065(2)	0.0064(2)	0.0012(1)	0.0036(1)	0.0010(1)
O(10)	0.39156(4)	0.36707(4)	0.60208(7)	0.00639(7)	0.0070(2)	0.0072(2)	0.0055(2)	-0.0018(1)	0.0030(1)	-0.0007(1)
O(11)	0.22615(4)	0.44667(4)	0.18277(7)	0.00711(7)	0.0087(2)	0.0059(2)	0.0071(2)	-0.0011(1)	0.0021(1)	0.0023(1)
O(12)	0.23591(4)	0.44861(4)	0.79057(7)	0.00594(7)	0.0058(2)	0.0054(2)	0.0065(2)	0.0012(1)	0.0001(1)	-0.0021(1)
H(1)	0.06558(9)	0.01328(10)	0.36283(15)	0.0214(2)	0.0184(4)	0.0214(4)	0.0232(4)	-0.0038(3)	-0.0016(3)	-0.0098(3)
H(2a)	0.46380(18)	0.10176(22)	0.69397(27)	0.0249(6)	0.0232(9)	0.0351(11)	0.0147(8)	-0.0035(7)	-0.0041(6)	0.0069(7)
H(2b)	0.4766(2)	0.0298(2)	0.5344(4)	0.0250(7)	0.0132(9)	0.0160(10)	0.0468(16)	0.0053(6)	0.0074(8)	0.0044(9)
H(3)	0.07060(11)	0.40794(12)	0.75715(18)	0.0299(2)	0.0329(5)	0.0313(5)	0.0266(5)	-0.0211(5)	0.0072(4)	-0.0090(4)
H(4)	0.04861(10)	0.04550(11)	0.82972(15)	0.0233(2)	0.0255(4)	0.0234(4)	0.0201(4)	0.0117(4)	-0.0003(3)	0.0032(3)

Note: Refined site occupancy factors of H(2a) and H(2b) are 0.546(6) and 0.446(6), respectively.

498

Table 4a. Principal root-mean-square components (R1, R2 and R3, x 10^2 Å) of the atomic displacement parameters based on the X-ray structure refinement.

Site	R1	R2	R3	R3/R3
Na	20.4(1)	13.0(1)	11.6(2)	1.76
Al(1)	8.2(1)	8.1(1)	6.5(2)	1.27
Al(2)	8.1(1)	7.5(1)	7.1(1)	1.14
Al(3)	8.1(1)	7.7(1)	6.3(2)	1.28
P(1)	7.8(1)	7.0(1)	6.48(8)	1.21
P(2)	7.4(1)	6.9(1)	6.40(8)	1.16
O(1)	9.6(3)	7.8(3)	6.9(4)	1.38
O(2)	9.2(3)	8.5(3)	8.0(3)	1.15
O(3)	9.9(2)	8.0(4)	7.4(3)	1.34
O(4)	9.5(3)	8.5(3)	7.5(3)	1.26
O(5)	10.9(3)	9.4(3)	7.5(3)	1.45
O(6)	8.9(3)	8.3(3)	8.0(3)	1.12
O(7)	9.4(3)	8.4(3)	7.0(4)	1.34
O(8)	10.5(2)	8.7(3)	7.4(3)	1.42
O(9)	10.4(2)	8.5(3)	7.1(4)	1.48
O(10)	10.6(2)	8.4(3)	6.9(4)	1.54
O(11)	10.5(2)	9.6(3)	7.8(4)	1.34
O(12)	9.6(3)	8.5(2)	7.8(3)	1.25

Table 4b. Principal root-mean-square components (R1, R2 and R3, x 10^2 Å) of the atomic displacement parameters based on the neutron structure refinement.

Site	R1	R2	R3	R1/R3
Na	19.9(1)	12.8(2)	11.3(2)	1.76
Al(1)	7.7(1)	6.9(1)	5.8(3)	1.32
Al(2)	7.2(2)	6.6(2)	5.3(2)	1.36
Al(3)	7.0(1)	6.4(2)	5.2(3)	1.35
P(1)	6.9(1)	5.8(2)	5.1(1)	1.34
P(2)	6.6(2)	5.5(2)	5.1(2)	1.29
O(1)	9.7(1)	6.2(2)	5.66(9)	1.71
O(2)	9.1(1)	6.93(7)	6.3(2)	1.43
O(3)	8.54(6)	7.5(1)	6.6(2)	1.30
O(4)	8.0(1)	7.8(1)	6.3(2)	1.26
O(5)	10.3(1)	8.2(1)	5.48(9)	1.89
O(6)	8.1(1)	7.5(1)	5.29(9)	1.52
O(7)	8.37(6)	7.1(1)	5.57(9)	1.50
O(8)	10.0(1)	8.4(1)	5.39(9)	1.87
O(9)	9.9(1)	7.6(1)	5.9(2)	1.67
O(10)	9.8(1)	7.7(1)	5.9(2)	1.67
O(11)	9.5(1)	9.4(1)	5.8(2)	1.64
O(12)	9.4(1)	7.42(7)	6.0(2)	1.58
H(1)	18.0(1)	14.8(1)	9.9(2)	1.82
H(2a)	19.9(3)	15.5(3)	10.5(4)	1.90
H(2b)	21.8(4)	13.6(3)	9.5(5)	2.30
H(3)	23.4(1)	15.7(2)	10.2(2)	2.30
H(4)	19.1(1)	14.9(2)	10.6(2)	1.79

Table 5. Relevant bond distances (Å) and angles (°) in the brazilianite structure based on the X-ray structure refinement (XSR) and the neutron structure refinement (NSR).

	XSR	NSR
Na – O(8)	2.432(1)	2.433(1)
Na – O(11)	2.450(1)	2.452(1)
Na – O(6)	2.526(1)	2.528(1)
Na – O(3)	2.581(1)	2.581(1)
Na – O(12)	2.631(1)	2.637(1)
Na – O(9)	2.642(1)	2.643(1)
Na – O(5)	2.728(1)	2.731(1)
Na – O(7)	2.909(1)	2.916(1)
Na – O(10)	3.106(1)	3.110(1)
<Na – O>	2.667	2.670
Al(1) – O(1)	1.809(1)	1.8106(9)
Al(1) – O(3)	1.841(1)	1.8464(9)
Al(1) – O(8)	1.864(1)	1.8620(9)
Al(1) – O(9)	1.877(1)	1.8794(9)
Al(1) – O(4)	1.954(1)	1.9536(9)
Al(1) – O(7)	2.125(1)	2.1242(9)
<Al(1) – O>	1.912	1.9127
Al(2) – O(1)	1.794(1)	1.7963(8)
Al(2) – O(2)	1.833(1)	1.8324(9)
Al(2) – O(11)	1.845(1)	1.8458(9)
Al(2) – O(12)	1.873(1)	1.8738(9)
Al(2) – O(7)	2.003(1)	2.0071(9)
Al(2) – O(6)	2.106(1)	2.1081(9)
<Al(2) – O>	1.909	1.9106
Al(3) – O(4)	1.853(1)	1.8541(9)
Al(3) – O(2)	1.877(1)	1.8825(9)
Al(3) – O(5)	1.883(1)	1.8787(9)
Al(3) – O(10)	1.895(1)	1.8923(9)
Al(3) – O(3)	1.932(1)	1.9333(9)
Al(3) – O(6)	2.025(1)	2.0275(9)
<Al(3) – O>	1.911	1.9114
P(1) – O(11)	1.523(1)	1.5256(7)
P(1) – O(5)	1.527(1)	1.5289(7)
P(1) – O(9)	1.540(1)	1.5386(7)
P(1) – O(6)	1.567(1)	1.5654(7)
<P(1) – O>	1.539	1.5396
P(2) – O(8)	1.523(1)	1.5251(7)
P(2) – O(10)	1.535(1)	1.5373(7)
P(2) – O(12)	1.537(1)	1.5386(7)
P(2) – O(7)	1.559(1)	1.5578(7)
<P(2) – O>	1.539	1.5397
O(1) – H(1)	0.974(1)	0.973(1)
O(1) – H(1)*		0.994
O(1)···O(4)	2.672(1)	2.673(1)
H(1)···O(4)	1.701(1)	1.703(1)
O(1) – H(1)···O(4)	174.1(1)	174.2(1)
O(2) – H(2a)	0.983(1)	0.984(1)
O(2) – H(2a)*		1.010
O(2)···O(9)	2.929(1)	2.933(1)
H(2a)···O(9)	2.031(1)	2.033(2)
O(2) – H(2a)···O(9)	151.0(1)	151.2(2)
O(2) – H(2b)	0.973(1)	0.970(1)
O(2) – H(2b)*		0.997
O(2)···O(2)	2.886(1)	2.881(1)
H(2b)···O(2)	1.922(1)	1.919(3)
O(2) – H(2b)···O(2)	170.8(1)	170.8(2)
O(3) – H(3)	0.968(1)	0.966(1)
O(3) – H(3)*		1.001
O(3)···O(12)	2.785(1)	2.788(1)
H(3)···O(12)	1.886(1)	1.889(1)
O(3) – H(3)···O(12)	153.3(1)	153.6(1)
O(4) – H(4)	0.967(1)	0.968(1)
O(4) – H(4)*		0.992
O(4)···O(10)	2.894(1)	2.898(1)
H(4)···O(10)	1.969(1)	1.972(1)
O(4) – H(4)···O(10)	159.4(1)	159.4(1)

* Bond distance corrected for "riding motion" following Busing and Levy (1964).

606 Fig. 1. Two views of the crystal structure of brazilianite (*i.e.* down [100] and [001])
607 based on the neutron structure refinement of this study. Thermal ellipsoid probability
608 factor: 60%. Al-octahedra are in light grey, P-tetrahedra in dark grey, Na sites (medium
609 grey) as un-bonded atoms, H-sites in white.
610
611

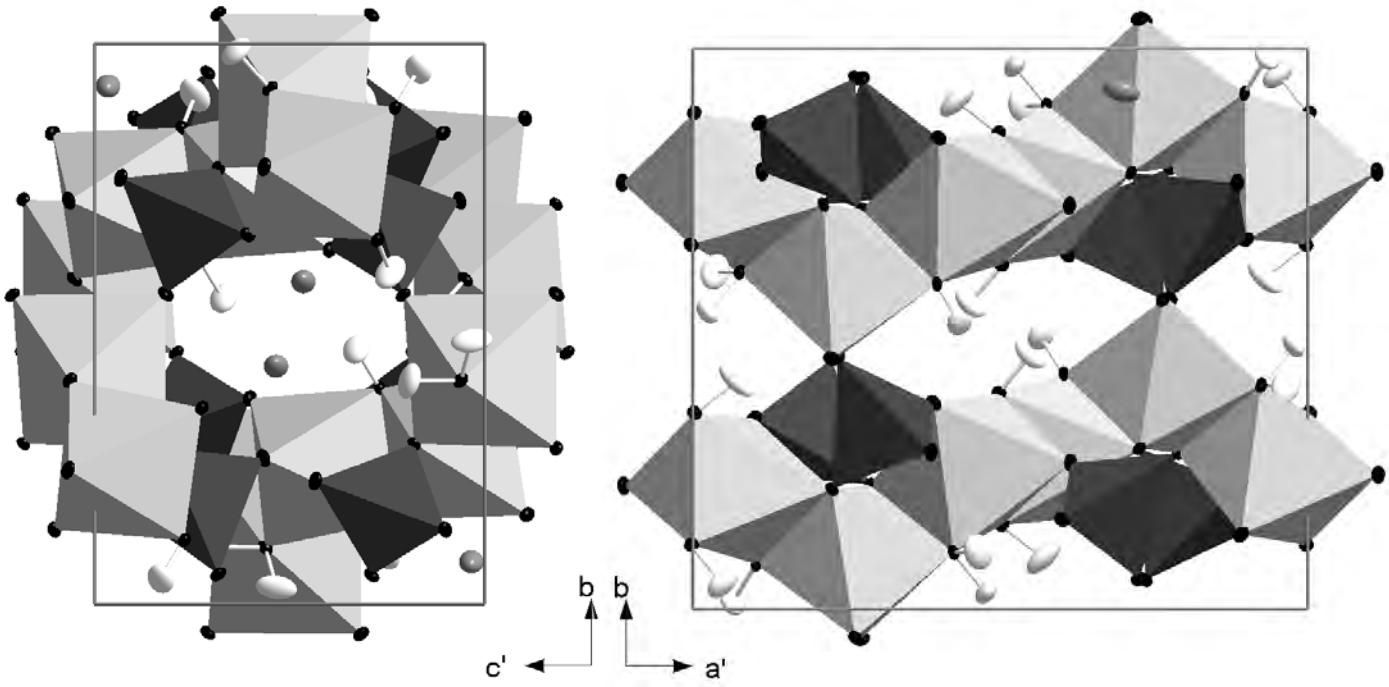

617
618
619
620
621
622
623
624
625
626
627

Fig. 2. Hydrogen sites location, H-bonding scheme and configuration of the Na-polyhedron in the structure of brazilianite based on the neutron structure refinement of this study. The sites H(2a) and H(2b) are mutually exclusive. Thermal ellipsoid probability factor: 60%.

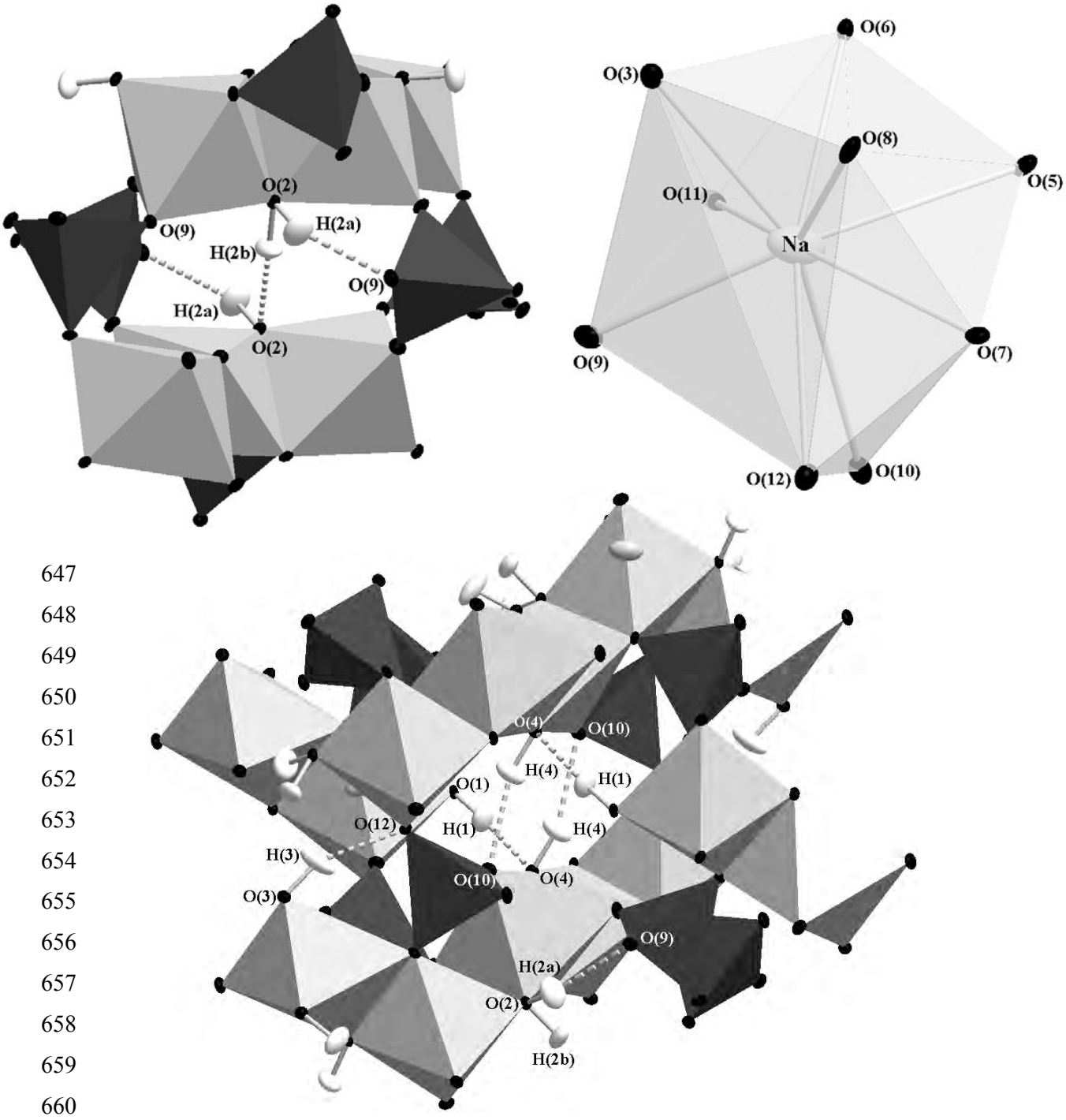

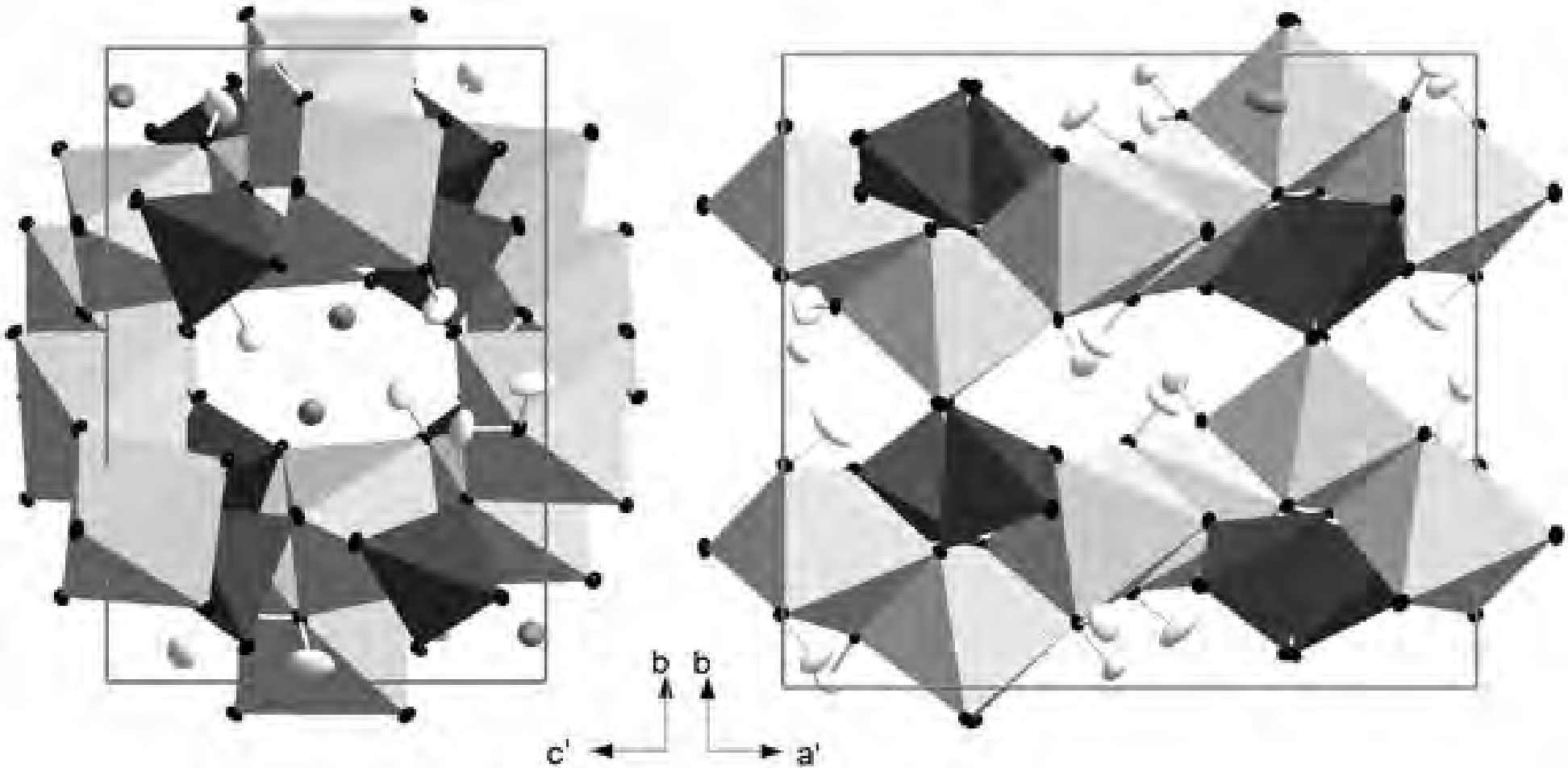
b
b
c'
a'

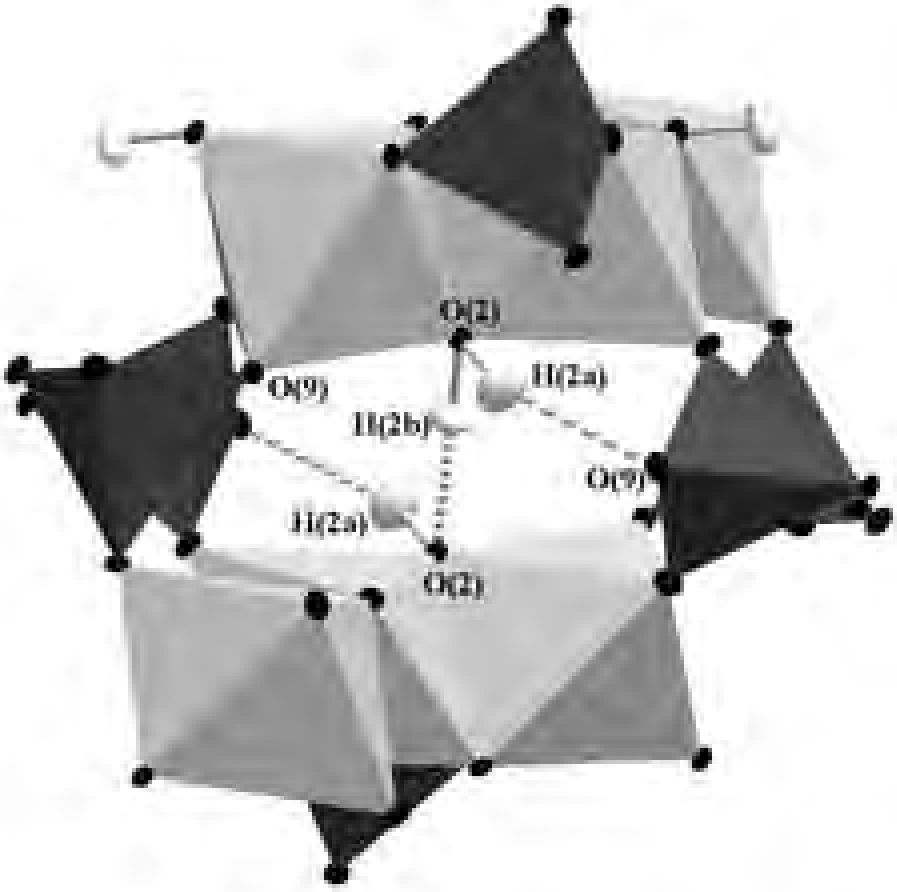
O(2)
O(9)
H(2a)
H(2b)
O(9)
H(2a)
O(2)

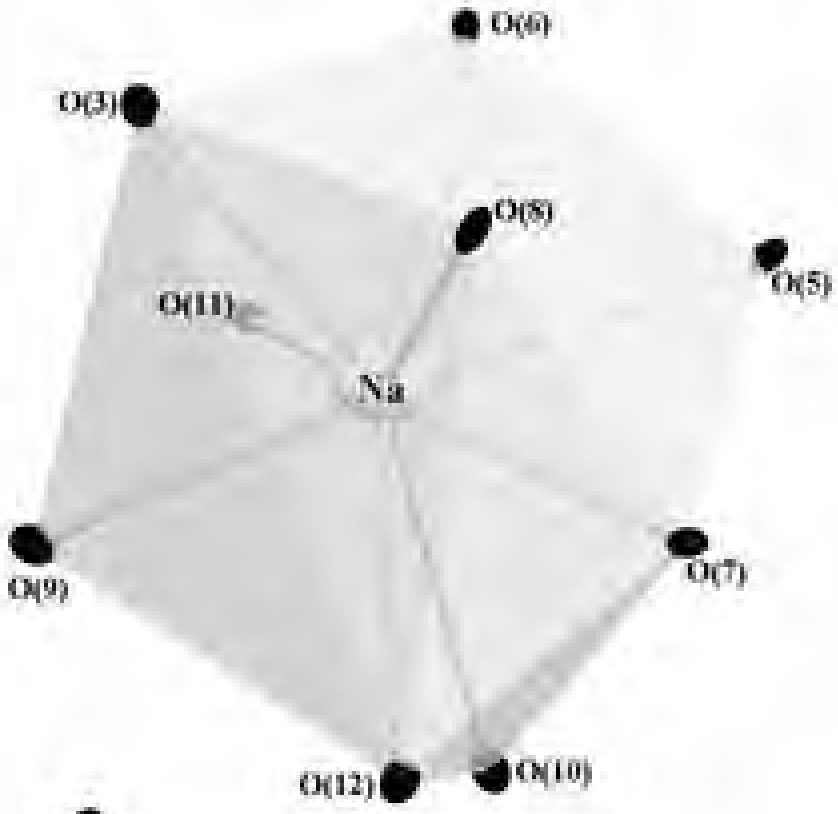
O(6)
O(3)
O(8)
O(5)
O(11)
Na
O(9)
O(7)
O(12)
O(10)

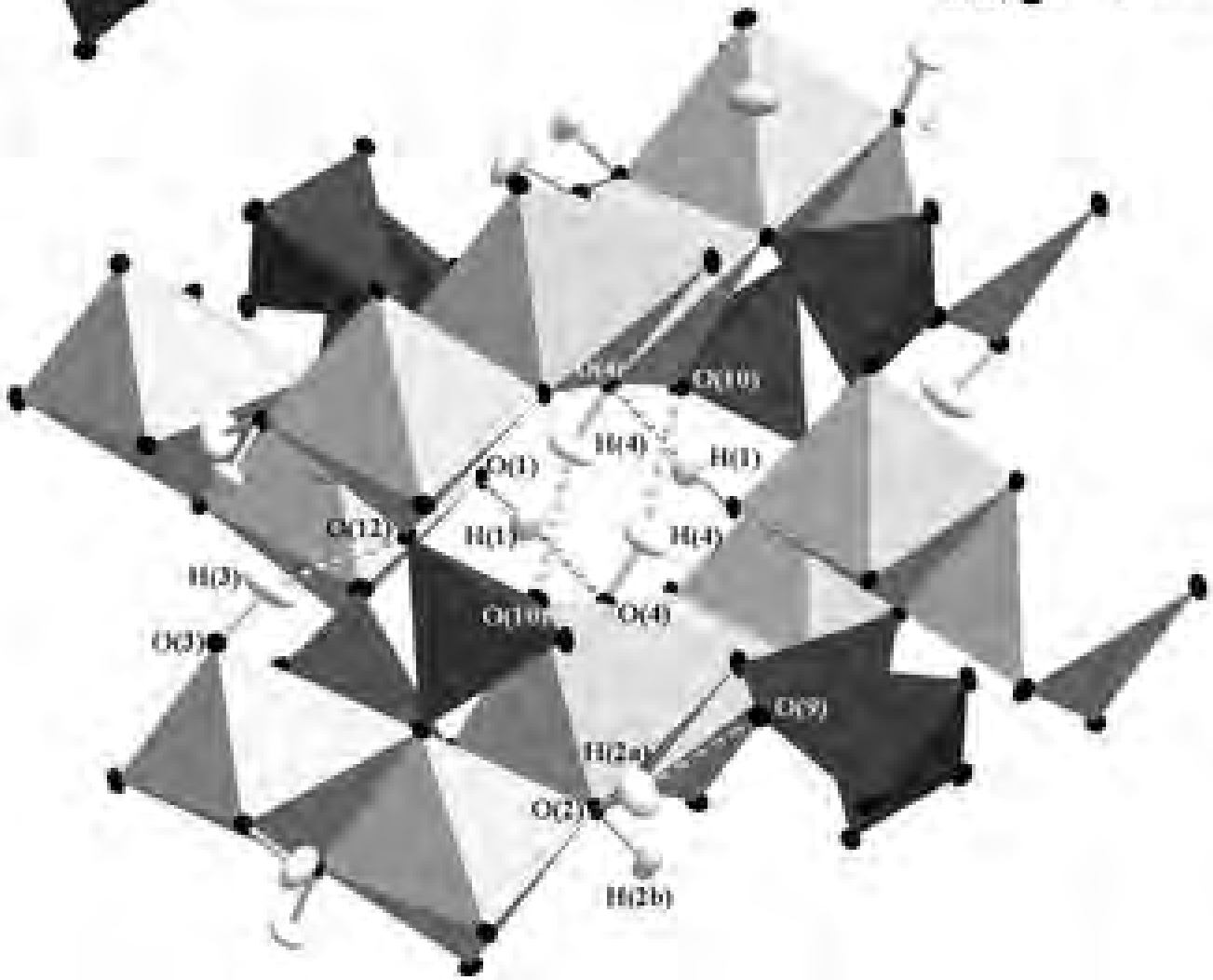
O(10)
H(4)
H(1)
O(1)
O(12)
H(1)
H(4)
H(3)
O(4)
O(3)
O(9)
H(2a)
O(2)
H(2b)